Journal of Engineering Sciences, Assiut University, Vol. 34, No. 2, pp. 519-538, March 2006

A NEW VOLTAGE COLLAPSE PROXIMITY INDICATOR

Dr. Gamal Abdelazim Mahmoud
Electrical Engineering Department, Faculty of Engineering , Suez Canal University, Port Said, Egypt

(Received January 21, 2006 Accepted February 23, 2006)

ABSTRACT– *Voltage stability problems have been one of the major concerns for electric utilities as a result of increase demanding of electric power. This paper develops a new voltage collapse proximity indicator using catastrophe theory together with comparative singularity of power flow Jacobian and modal analysis. The application of the proposed indicator has been demonstrated on multimachine power systems.*

KEYWORDS: *Voltage stability criteria, Catastrophe theory, Jacobian matrix, Modal analysis*.

1 - INTRODUCTION

Recently a number of utilities in different countries throughout the world have experienced voltage collapse problems. In some cases blackouts occurred as a result of voltage collapse [1-4] . Part of the reason for these types of problems is that today's power system utilities are highly stressed and heavily loaded without an adequate corresponding increase in the system capacity.

The problem of collapse may be simply explained by an inability of the power system to supply the reactive power or by an excessive absorption of reactive power by the system itself. Reactive power problems arise in power systems under a Varity of conditions. For lightly loaded system, too much reactive power may be injected into the network by shunt elements resulting in overly high voltages at the voltage uncontrolled buses. Alternatively, under heavy load conditions, there may be insufficient injected reactive power causing the voltage to drop. In some cases heavily loaded power systems, particularly when the system configuration comprises long transmission lines, the voltage drop caused by the dropping of a generator or a transmission line cannot be recovered even if the static capacitors at load ends are switched on. This type of abnormal voltage rapid fall is called voltage instability or voltage collapse phenomena. There are two general types of tools for voltage stability analysis: dynamic and static. Dynamic analysis uses time-domain simulation to solve nonlinear system differential / algebraic equations. Static analysis is based on the solution of conventional or modified power flow equations.

Dynamic analysis provides the most accurate replication of the time responses of power system [5] . Accurate determination of the time sequence of the different events loading to system voltage instability is essential for post-disturbance analysis

and the coordination of protection and control. However , time-domain simulations are time consuming in terms of CPU and engineering required for analysis of results. Also, dynamic analysis does not readily provide information regarding the sensitivity of degree of instability. These limitations generally make dynamic analysis impractical for examination of a wide range for system conditions for determining stability limits.

Static analysis [6] involves only the solution of power flow equations and therefore is computationally much more efficient than dynamic analysis. Several algorithms have been developed to study the steady-state (static) voltage instability. The minimum singular value of the system Jacobian matrix has been proposed as a voltage collapse index [7]. However calculating the minimum singular value is time consuming due to the high dimension of the Jacobian matrix. To improve the feasibility of this method, a fast algorithm to compute the minimum singular value was proposed [8]. Modal analysis also reported for voltage instability assessment [9]. This method calculates a set of the smallest eigenvalues of the reduced Jacobian matrix and the associated participation factors. The eigenvalues are used as voltage instability indicators and the participation factors for weak area identifications. Voltage – Power (real or reactive) sensitivity is another index for voltage collapse detection . During normal operating conditions, the Voltage – Power sensitivity is a finite value, and it will increase with the system loading .When voltage collapse occurs, the Voltage – Power sensitivity will be infinite [10]. Another developed method using the distance in the load parameter space between a given operating condition and the critical point, which is the voltage collapse point, as index .Algorithms for calculating this distance were further investigated , while this index can provide a load power margin for an operating condition, which is particularly valuable to system operators, the computational burden is a main concern [11].

The study of this phenomena could be put into framework of catastrophe theory which describes how sudden jumps in the system states can arise from a smooth change of the system parameters [12]. The voltage stability manifold is defined as an equilibrium surface of critical points . It can be obtained by deriving the minimum of the system function which involves voltage and system parameters as state and control variables respectively. In reference [13] , the theory was applied on a simple system consisting of a single generator supplying a static load through a lossless transmission line. The control parameter ($a < 0$) was used as an indicator for voltage stability index.

In this paper, an attempt has been made to find a physical explanation for voltage instability phenomena in interconnected multi-machine system using the catastrophe theory together with comparative singularity of power flow Jacobian and modal analysis . The study is based on the analysis of the phenomena under the effects of changing the system parameters.

2 - CATASTROPHE THEORY

In any system (physical or natural) if some of the parameters of that system continue to vary very smoothly, a critical stage may be reached at which point the system exhibits a sudden jump from state to another. The other state may be different from the original state. Power system like many of the most interesting phenomena in nature involves discontinuities. One of the reasons for these discontinuities is the

voltage collapse. Catastrophe theory tries to deal with the properties of these discontinuities.

Consider a gradient system whose behavior is usually smooth, but sometimes (or in some places) exhibits discontinuation and described by a potential function E_p with n state variables (X_1,.., X_i,…, X_n) and m control variables (C_1,..., C_k,., C_m) . Then the equilibrium equations are given by:

$$\frac{\partial E_p}{\partial X_i} = 0 \qquad i = 1, \ldots\ldots\ldots, n \tag{1}$$

Define an m-dimensional equilibrium surface in the (n + m) dimensional space spanned by the X_i and C_k. Since the potential depends upon the control parameters, The Hessian of E_p and its eigenvalues also depend on these control parameters. For certain values of control parameters, one or more of these eigenvalues may assume the value zero. When this happens, the Hessian of E_p is

$$\det\left[\frac{\partial^2 \mathrm{Ep}}{\partial X_i \partial X_j}\right] = \det\left[\mathrm{Ep}_{ij}\right] = 0 \tag{2}$$

and the system critical points are called non-isolated degenerate or non-Morse critical points at which the system exhibits instability, but when the det $[\mathrm{Ep}_{ij}] \neq 0$, the critical points are called isolated non-degenerate or Morse critical points at which the system is stable. Therefore the system potential function E_p can be split into parts (stable/unstable part). This is called splitting lemma [14-16], because it allows us to split the critical point into two parts: part involved in structural stability (non-degenerate associated with the non-vanishing eigenvalues), and the other involved in instability(degenerate associated with the vanishing eigenvalues).

According to Thom's theorem, in an open neighborhood of a critical point (where ℓ eigenvlaues vanish), the original potential function E_p can be written in the canonical form.

$$E_p = \mathrm{Cat}(\ell\ , m) + \sum_{j=l+1}^{n} \lambda_j y_j^2 \tag{3}$$

Where, $\mathrm{Cat}(\ell\ , m)$ is the catastrophe function
λ_j is the number of non-zero eigenvalues
y_j is the coordinates associated with non-vanishing eigenvalues

The catastrophe function $\mathrm{Cat}(\ell,m)$ gives the qualitative configurations of the system discontinuities that occur in the neighborhood of critical points. The second term in equation 3 does not contribute for discontinuities and can be ignored in the analysis.

According to Thom's classification theory, in any system governed by a potential function, and in which the system behavior is determined by no more than four different control variables, only seven qualitative different types of catastrophe functions are possible and given in **Table 1**. These are called elementary catastrophes.

Table 1: Seven elementary Catastrophes.

Catastrophe Manifold	Control variable	State variable	Function	Derivative
Fold	1	1	$x^3/3 + a\,x$	$x^2 + a$
Cusp	2	1	$x^4/4 + b\,x^2/2 + ax$	$x^3 + b\,x + a$
Swallowtail	3	1	$x^5/5 + a\,x^3/3 + bx^2/2 + cx$	$x^4 + ax^2 + bx + c$
Butterfly	4	1	$x^6/6 + a\,x^4/4 + b\,x^3/3 + cx^2/2 + dx$	$x^5/5 + a\,x^3/3 + bx^2/2 + cx$
Hyperbolic	3	2	$x^3 + y^3 + axy + bx + cy$	$3x^2+ay+b+3y^2+ax+c$
Elliptic	3	2	$x^3 + a(x^2+ y^2) -3xy + bx + cy$	$3x^2-3y^2+2ax+b-6xy+2ay+c$
Parabolic	4	2	$X^2y + y^4 + ax^2 + by + cx+dy$	$2xy+2ax+c+x^2+4y^3+2by+d$

3 - PROBLEM FORMULATION

As mentioned in the last paragraph of the introduction, the voltage collapse phenomena needs more explanation for voltage instability. The basic configuration used to explain voltage collapse is shown in **figure 1-a**. In this circuit the voltage source E_{th} in series with the equivalent transmission impedance Z_{th} represents the Thevenin equivalent of a network connected to a load. The load is described by its real and reactive powers as shown.

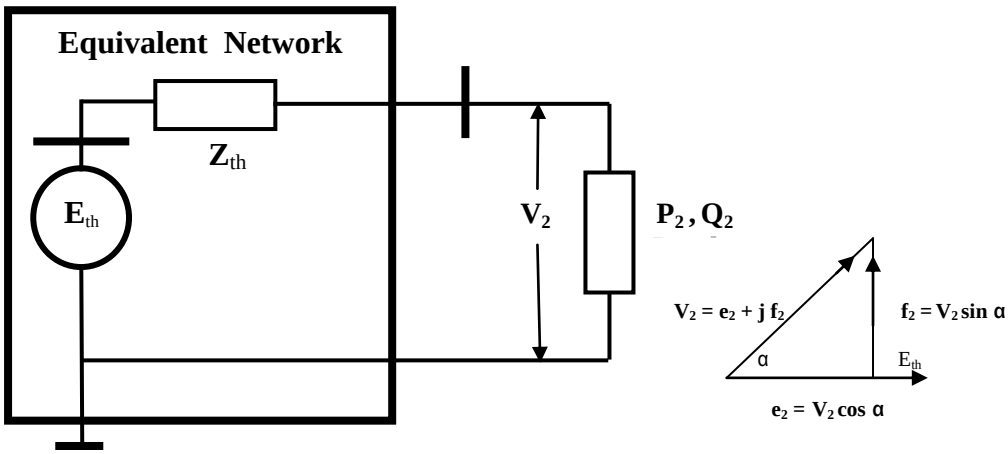

Figure 1.a: Thevenin Equivalent Network.

The load receiving end voltage V_2 in terms of P_2 and Q_2 and the Z_{th} is obtained as follows [17]:

$$V_2 = E_{th} - \frac{S_2^* Z_{th}}{V_2^*} \tag{4}$$

Therefore,

$$E_{th}V_2^* = V_2V_2^* + S_2^*Z_{th} \tag{5}$$

Where,

$V_2 = |V_2| \angle \alpha$, $E_{th} = |E_{th}| \angle 0$, $S_2 = P_2 + j\, Q_2$ *and* $Z_{th} = R_{th} + j\, X_{th}$

Rewrite eqn.(5) in terms of real and imaginary components:

$$V_2 E_{th} \cos \alpha = V_2^2 + (P_2 R_{th} + Q_2 X_{th})$$
$$V_2 E_{th} \sin \alpha = - (P_2 X_{th} - Q_2 R_{th}) \quad (6)$$

Equations (6) represent the PV relationship and **figure 1-b** shows this for 2-bus network. For a constant power demand, there exists two operating points except the saddle point which represents the steady state stability limit. The higher operating voltage is called the stable operating point and is the feasible solution. On the contrary, the lower one is the unstable point and is infeasible [18]. In this paper, it will be shown that the higher operating point has positive value of the new proposed indicator using Catastrophe theory, the Jacobian matrix determinant, and the Eigenvalue of the reduced Jacobian matrix and lower one is negative for them. The determinant approaches zero if the operating move to the saddle point.

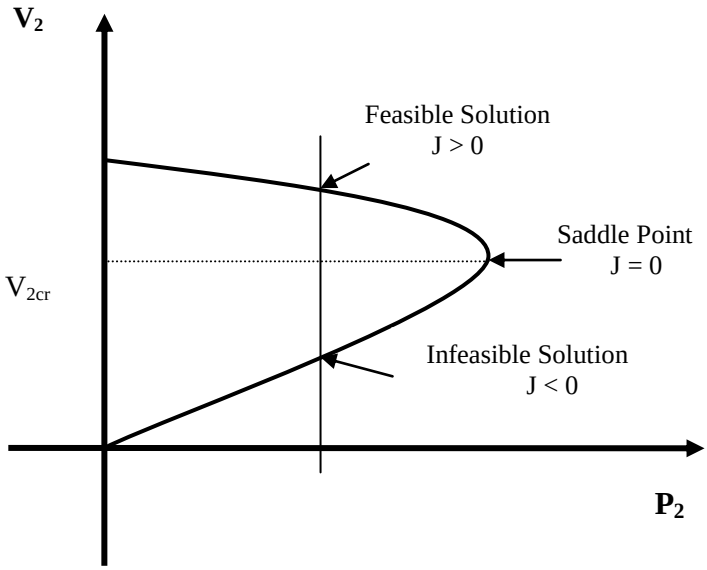

Figure 1-b: Receiving Power vs. Load Voltage for two-node Network.

Since short circuit capability equals Scc = $\frac{E^2_{th}}{Z_{th}}$, then dividing both sides of equations (6) by Scc, we obtain the following equations:

$$f = -(PX_{th} - QR_{th}) / Z_{th}$$
$$and \quad (7)$$
$$e = V^2 + (P\, R_{th} + Q\, X_{th})$$

where,

$$e = \frac{V_2 \cos\alpha}{E_{th}}, f = \frac{V_2 \sin\alpha}{E_{th}}, P = \frac{P_2}{SCC}, Q = \frac{Q_2}{SCC}, and\ V = e + jf$$

Squaring and adding eqns (7), we obtain the following equation:

$$V^4 + V^2\left(\frac{2(PR_{th} + QX_{th})}{Z_{th}} - 1\right) + (P^2 + Q^2) = 0 \tag{8}$$

or,

$$V^4 + aV^2 + bV + c = 0 \tag{9}$$

where,

$$a = \frac{2(PR_{th} + QX_{th})}{Z_{th}} - 1$$

$$b = 0$$

$$c = (P^2 + Q^2)$$

Equation (9) is seen to be the swallowtail catastrophe manifold, with load bus voltage as a state variable and control variables a, b = 0, and c represent the system parameters . As seen the control variables depend upon the load active and reactive components as well as the system equivalent Thevenin impedance. Eqn (9) has the solution in V^2 as:

$$V^2 = \left(\frac{-a}{2} \pm \sqrt{(a/2)^2 - c}\right) \tag{10}$$

3.1 The Critical Voltage of Loading Node

Next, we find the singularity set S which is the subset of the catastrophe manifold equation (9) that consists of all singular points corresponding to the system critical voltage stability. These are the points at which the first derivative of equation (9) equal to zero, as follows:

$$4V^3 + 2aV = 0$$

$$or \tag{11}$$

$$V_{cr} = \pm\sqrt{\frac{-a}{2}}$$

It is clear that for stable operation , the control parameter **a** should be less than zero, and

$0 < c < \left(\frac{a}{2}\right)^2$ to get real solution and is considered here a new indicator for voltage stability. The indicator can now be determined for each load bus in the power system. The weakest bus in the system will have the smallest magnitude for the indicator **c** as well as the smallest eigenvalue of the Jacobian J_x indicating that the system is on the verge of instability.

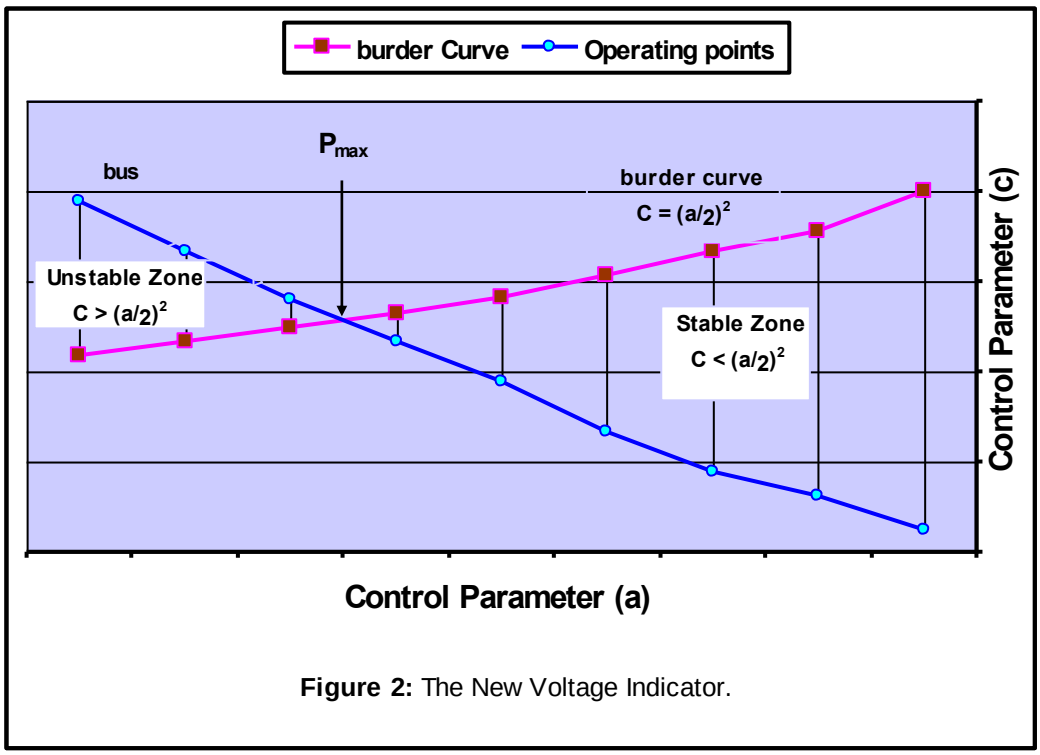

Figure 2: The New Voltage Indicator.

The singularity set S is then projected down onto a two-dimensional control space (**a,c**) to obtain the bifurcation set **β** . The bifurcation set is the image of catastrophe manifold in the control space which provides the region of all possible stable voltage operations in terms of the control variables (**a, c**), which usually represent the system parameters as illustrated in **figure 2**.

By substituting equation (7) at critical operation into equation (11), we obtain the value of critical voltage:

$$V_{cr} = \frac{E_{th}}{2\cos\alpha} \tag{12}$$

3.2 The Maximum Power Loading

Corresponding to maximum loading, there is one value of V_{cr} as the two values are superimposed, then the term under the root of equation (10) must vanishes, i.e, the term under the root becomes zero, then,

$$c = \left(\frac{a}{2}\right)^2$$
$$or \tag{13}$$
$$P^2 + Q^2 = \left(\frac{PR_{th} + QX_{th}}{Z_{th}} - \frac{1}{2}\right)^2$$

Equation (13) can be rewritten in the general form as :

$$LP^2 + KP + M = 0 \tag{14}$$

P in equation (14) is P_{max} of the node under study. Solution of equation (14) results in two values of P, one of them is negative and the other is positive. Evidently the positive value should be considered. Therefore,

$$P_{\max} = (\frac{1}{2L})(-K \pm \sqrt{K^2 - 4LM}) \tag{15}$$

where,

$$L = 1$$

$$K = \frac{-R_{th}(2QX_{th} - Z_{th})}{X^2}$$

$$M = (\frac{R_{th}Q}{X_{th}})^2 + \frac{QZ_{th}}{X_{th}} - (\frac{Z_{th}}{2X_{th}})^2$$

As seen the presence of a reactive component of load Q and system impedance affects the loading power limit.

4 - VOLTAGE STABILITY EVALUATION USING JACOBIAN MATRIX ELEMENTS

The use of the singularity of power flow Jacobian matrix as an indicator of steady state stability was first pointed out by reference [19] , where the sign of the determinant of J_x was used to determine if the studied operating point was stable or not.
From energy conservation, the following active and reactive load flow equations for P and Q can be obtained from equations (7) and taken negative (injected at load bus):

$$-P = \frac{R_{th}}{Z_{th}}(e - V^2) - \frac{X_{th}f}{Z_{th}} \tag{16}$$

$$-Q = \frac{X_{th}}{Z_{th}}(e - V^2) + \frac{R_{th}f}{Z_{th}} \tag{17}$$

From the linearized Power flow equations (16) and (17) we obtain

$$\begin{pmatrix} \Delta P \\ \Delta Q \end{pmatrix} = \begin{pmatrix} \frac{\partial P}{\partial f} & \frac{\partial P}{\partial e} \\ \frac{\partial Q}{\partial f} & \frac{\partial Q}{\partial e} \end{pmatrix} \begin{pmatrix} \Delta f \\ \Delta e \end{pmatrix} \tag{18}$$

where, the elements of the Jacobian matrix of the system is

$$\frac{\partial P}{\partial f} = (X_{th}+2R_{th}f)/Z_{th} \quad , \quad \frac{\partial P}{\partial e} = R_{th}(2e-1)/Z_{th}$$

$$\frac{\partial Q}{\partial f} = (2X_{th}f - R_{th})/Z_{th} \quad , \quad \frac{\partial Q}{\partial e} = X_{th}(2e -1)/Z_{th}$$

and the determinant of the Jacobian matrix is

$$| J_x | = Z_{th}(2e - 1) \tag{19}$$

The singular points corresponding to the system critical voltage stability occur when the determinant of the Jacobian matrix is zero. Then at $| J_x | = 0$, we obtain

$$e_{cr} = ½ \tag{20}$$

or

$$V_{cr} = \frac{E_{th}}{2\cos\alpha} \tag{21}$$

Equation (21) represents the critical load bus voltage and as seen the same equation obtained using the catastrophe theory (equation (12)). After a little manipulation for equations (16) and (17) we have:

$$\begin{aligned} &(e-\frac{1}{2})^2 + (f+\frac{X_{th}}{2R_{th}})^2 = (\frac{Z_{th}^2 - 4R_{th}Z_{th}P}{4R^2}) \\ &and \\ &(e-\frac{1}{2})^2 + (f+\frac{R_{th}}{2X_{th}})^2 = (\frac{Z_{th}^2 - 4X_{th}Z_{th}Q}{4X^2}) \end{aligned} \tag{22}$$

where, the value of f is given in equation (7) and the value of e is recalculated and given by:

$$e = \frac{1}{2} \pm \sqrt{\frac{1}{4} - \frac{1}{Z_{th}^2}[(X_{th}P - R_{th}Q)^2 + Z_{th}(R_{th}P + X_{th}Q)]} \tag{23}$$

Equations (22) define two circles on (e–f) plane Shown in **figure 3**, with centers at $(\frac{1}{2}, \frac{-X_{th}}{2R_{th}}), (\frac{1}{2}, \frac{R_{th}}{2X_{th}})$ and radiuses of $\sqrt{\frac{Z_{th}^2 - 4R_{th}Z_{th}P}{4R_{th}^2}}$ and $\sqrt{\frac{Z_{th}^2 - 4X_{th}Z_{th}Q}{4X_{th}^2}}$

respectively. The radiuses vary with the real and reactive load respectively. The heavier the load is, the smaller the radiuses will be. The intersection points define the possible values of voltages (e , f) at the load bus.

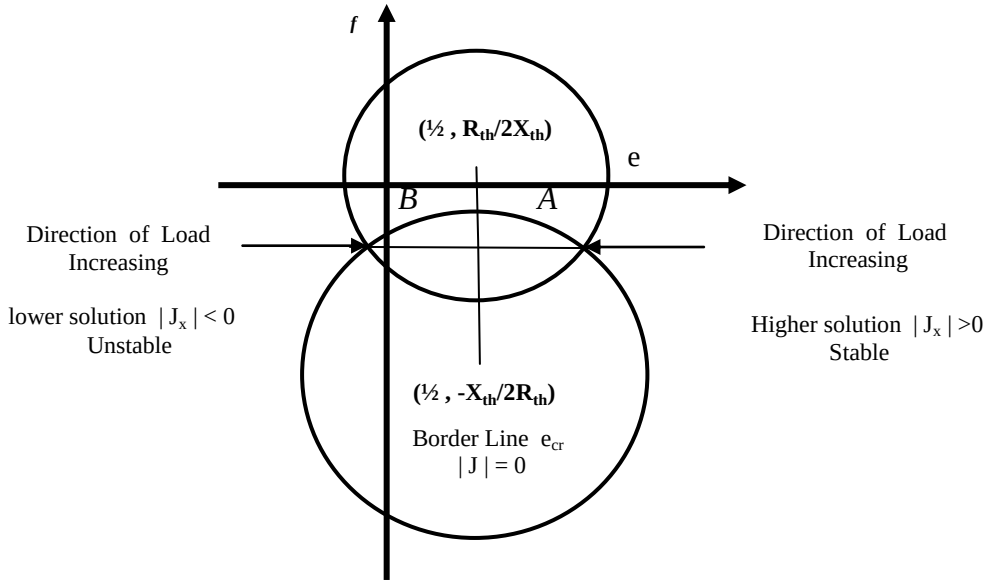

Figure 3: Load Bus Voltage Solutions.

From **figure 3**, it is clear that there are two solutions (higher and lower) for the load bus voltage (*e , f)* as long as $\frac{X_{th}P - QR_{th}}{Z_{th}}$ is less than the radius of the circle. Also to get the real roots for *e* , we have:

$$(X_{th}P - R_{th}Q)^2 + Z_{th}(R_{th}P + X_{th}Q) \le (\frac{Z_{th}}{2})^2 \qquad (24)$$

Equation (20) represents the vertical line connects the centers of the circles defined by equations (22). This line can be considered as the border between the stable (area A right hand side) and unstable (Area B left hand side) areas in the voltage plane, which is similar to the border curve obtained at $V_{cr} = \frac{E_{th}}{2\cos\alpha}$ or at e_{cr} = ½ from the catastrophe theory .

5 - VOLTAGE STABILITY EVALUATION USING MODAL ANALYSIS

Voltage stability characteristics of the system can be identified by computing the eigenvalues of the reduced Newton-Raphson load flow Jacobian matrix. The linearized steady-state system power voltage equations are illustrated in equation (18) and the variation in reactive load flow ΔQ at constant active power component (i.e ΔP = 0) is given by:

$$\Delta Q = (J_{Q_e} - J_{Q_f} J_{p_f}^{-1} J_{p_e})\Delta e$$

or

$$\Delta Q = J_{xR}\Delta e \qquad (25)$$

where,

$$J_{xR} = (J_{Q_e} - J_{Q_f} J_{p_f}^{-1} J_{p_e})$$

$J_{pf} = (X_{th}+2R_{th}f)/Z_{th}$, $J_{pe} = R_{th}(2e-1)/Z_{th}$

$J_{Qf} = (2X_{th}f - R_{th})/Z_{th}$, $J_{Qe} = X_{th}(2e -1)/Z_{th}$

J_{xR} is a reduced Jacobian matrix of two node system, and its dimension is 1 x 1 matrix. Eigenvalue of this reduced Jacobian matrix is used as indicator of voltage stability. If the eigenvalue of J_{xR} is positive, the system is considered voltage stable. The system is considered voltage unstable if the eigenvalue of J_{xR} is negative . At each operating point we keep the active power component constant and evaluate voltage stability by considering the incremental relationship between the reactive power Q and the magnitude of active bus voltage e.

6 – NUMERICAL EXAMPLE

In order to study the intrinsic characteristics of the catastrophe control parameters (a, c), the singularity of power flow through the determinant sign of the Jacobian matrix and the eigenvalue of the reduced Jacobian matrix using modal analysis and their relations to voltage instability state, a theoretical test system has been adopted. The test system is the Ward-Hale 6-bus Network [20] shown in **figure 4**. This system, generally used for testing the new developed techniques in comparison to the known ones. The initial data for generation and load of the system is given in **Table 2**. The results of the conventional load flow run of the test system are shown in **Table 3**. In this run, bus 1 is taken as the slack bus and bus 2 is maintained at constant voltage of 1.1 p.u. An accuracy of 0.00001 was achieved in both voltage magnitude and angle.

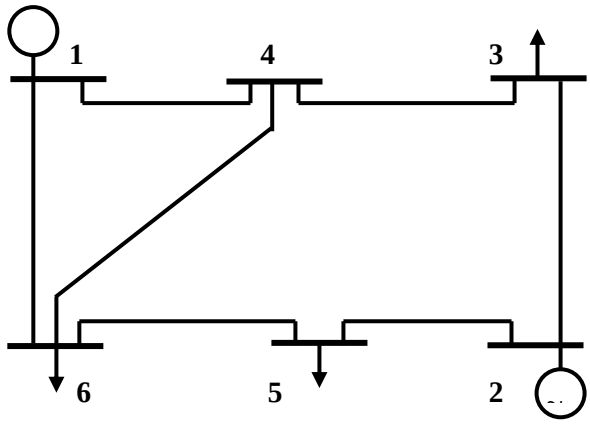

Figure 4: Ward-Hale 6-bus Network.

Table 2: Bus Loading and Voltages.

Bus Number	Bus Voltage	Active Power	Reactive Power
1	1.050	……	……
2	1.100	0.500	……
3	……	- 0.550	- 0.13
4	……	- 0.000	- 0.000
5	……	- 0.300	- 0.18
6	……	- 0.500	- 0.05

For this system, the Thevenin's equivalent (E_{th} and Z_{th}) at each load node with its load separated is firstly calculated. The Thevenin's p.u. voltages E_{th} and impedances Z_{th} for the load nodes (nodes 3 – 6) are found to be as given in **Table 4**.

Table 3: Load Flow Results.

Bus Number	Bus Voltage	Active Power	Reactive Power
1	$1.050 \angle 0$	0.952	0.433
2	$1.100 \angle -3.34$	0.500	0.184
3	$1.0008 \angle -12.78$	- 0.550	- 0.13
4	$0.9290 \angle -9.84$	0.000	0.000
5	$0.9198 \angle -12.33$	- 0.300	- 0.18
6	$0.9192 \angle -12.24$	- 0.500	- 0.05

Table 4: Thevenin's equivalents.

Bus Number	Thevenin's Voltage Eth	Thevenin's impedance Zth
3	$0.975 \angle -1.023$	$0.2740 \angle 75.64$
4	$0.954 \angle -9.93$	$0.2220 \angle 75.81$
5	$1.000 \angle -3.1987$	$0.32315 \angle 75.43$
6	$0.987 \angle -3.21$	$0.2370 \angle 75.54$

The new indicator c , the singular value of the Jacobian $|\mathbf{J_x}|$ and the eigenvalues λ using modal analysis are applied and calculated for each load node at the nominal load setting. In order to test these indicators, two tests are carried out :

6.1 The First Test

Stressing each load node of the test Ward-Hale 6-bus Network with keeping the reactive power constant at each load node by gradually increases the active power, starting from the base load up to 130% P_{max} . The results show complete agreement, also, it shows the value of the critical voltage V_{cr} for each load node and its corresponding consumed max power $P_{max.}$. The criteria for the system to be stable, the new indicator c should be less than $(a/2)^2$, the determinant values of the Jacobian $|\mathbf{J_x}|$ and the eigenvalues λ also should be positive values as shown in **Table 5**. The new

indicator c using the catastrophe theory provides a way to determine the stable and unstable zones as shown in **figure 5**. As seen the break away point which represents the critical loading point at each bus occurs at loading with maximum value. This point corresponding to the saddle point obtained from P-V relationship as shown in **figure 1-b** which separates between the stable and unstable zones.

Table 5-a: The New and Different Voltage Stability Indicators for Load Bus 3 for 6 – Bus Power System.

Bus Number	New indicator		Jacobian Value $\lvert J_x \rvert$	Eigenvalue λ	Critical Voltage V_{cr}	Bus Loading	System State
	c	A					
BUS 3 Maximum Loading p.u 1. 2289	0.0265	-0.8319	0.2097	3.3350	0.629	Base Load	Stable
	0.0327	-0.8205	0.2018	3.2540	0.625	50% P_{max}	Stable
	0.0465	-0.7987	0.1842	3.0559	0.616	60% P_{max}	Stable
	0.0719	-0.7663	0.1500	2.6074	0.604	75% P_{max}	Stable
	0.1.03	-0.7340	0.9751	1.8067	0.591	90% P_{max}	Stable
	0.1268	-0.7122	0.0000	0.1219	0.582	100% P_{max}	Critical Stable
	0.1532	-0.6908	-0.41100	-7.403087	0.573	110% P_{max}	Unstable
	0.1820	-0.6690	-0.41100	-7.624514	0.564	120% P_{max}	Unstable
	0.2134	-0.6475	-0.41100	-7.859595	0.555	130% P_{max}	Unstable

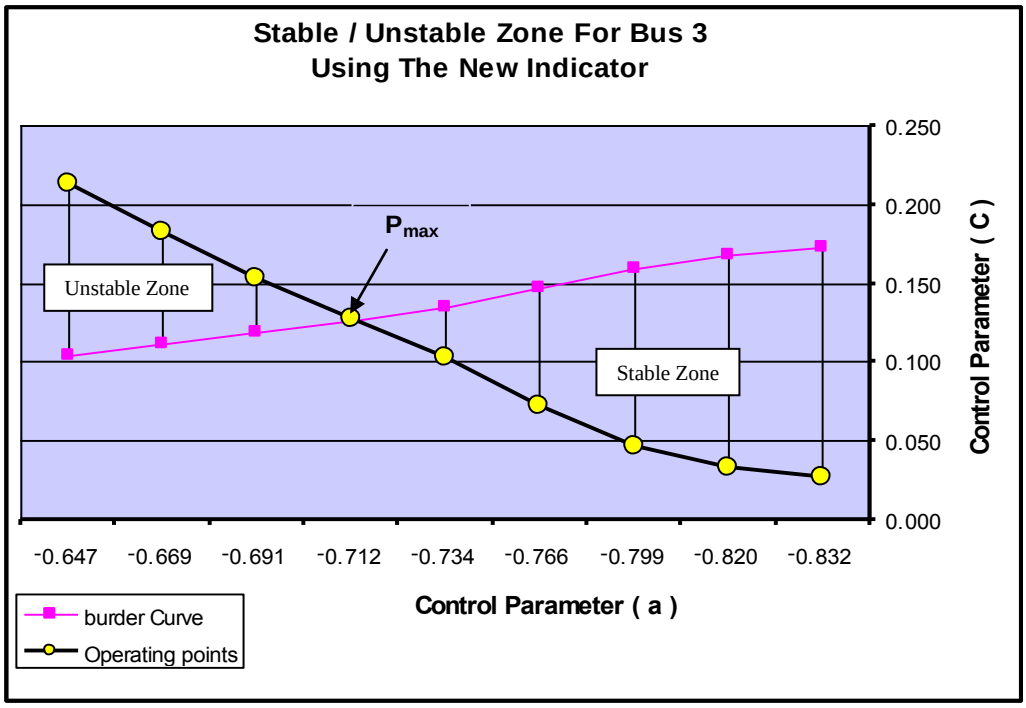

Figure 5-a: Operating Zones for Bus 3.

Table 5-b: The New and Different Voltage Stability Indicators for Load Bus 4 for 6 – Bus Power System.

Bus Number	New indicator		Jacobian Value $\lvert J_x \rvert$	Eigenvalue λ	Critical Voltage V_{cr}	Bus Loading	System State
	c	A					
BUS 4 Maximum Loading p.u 1. 573	0.0000	-1.000	0.222	4.943280	0.674580	Base Load	Stable
	0.0368	-0.900	0.17595	4.531556	0.634206	50% P_{max}	Stable
	0.0530	-0.860	0.16139	4.277920	0.625819	60% P_{max}	Stable
	0.0828	-0.826	0.13414	3.688300	0.613023	75% P_{max}	Stable
	0.1193	-0.791	0.85462	2.608000	0.599955	90% P_{max}	Stable
	0.1473	-0.768	0.00000	0.287339	0.591082	100% P_{max}	Critical Stable
	0.1783	-0.744	-0.333000	-9.384356	0.582073	110% P_{max}	Unstable
	0.2122	-0.721	-0.33300	-9.707075	0.572923	120% P_{max}	Unstable
	0.2490	-0.698	-0.33300	-10.05278	0.563625	130% P_{max}	Unstable

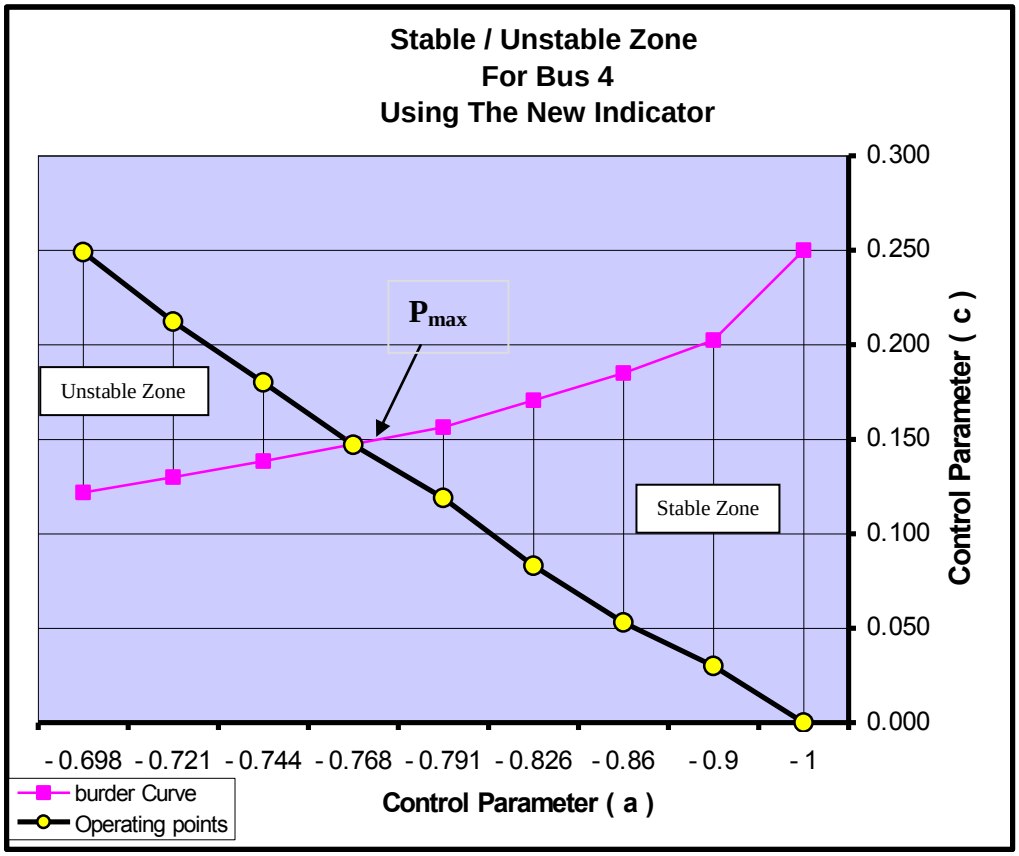

Figure 5-b: Operating Zones for Bus 4.

Table 5-c: The New and Different Voltage Stability Indicators for Load Bus 5 for 6 – Bus Power System.

Bus Number	New indicator		Jacobian Value $\lvert J_x \rvert$	Eigenvalue λ	Critical Voltage V_{cr}	Bus Loading	System State
	c	a					
BUS 4 Maximum Loading p.u 1. 0398	0.0104	-0.8787	0.276166	2.936918	0.663	Base Load	Stable
	0.0316	-0.7856	0.226402	2.510242	0.627	50% P_{max}	Stable
	0.0440	-0.7647	0.206671	2.345026	0.618	60% P_{max}	Stable
	0.0668	-0.7337	0.168214	1.977991	0.606	75% P_{max}	Stable
	0.0948	-0.7025	0.109354	1.334347	0.593	90% P_{max}	Stable
	0.1162	-0.6817	0.000000	0.000000	0.584	100% P_{max}	Critical Stable
	0.1399	-0.6612	-0.161575	-2.013231	0.575	110% P_{max}	Unstable
	0.1659	-0.6403	-0.161575	-2.066252	0.566	120% P_{max}	Unstable
	0.1941	-0.6197	-0.161575	-2.122141	0.557	130% P_{max}	Unstable

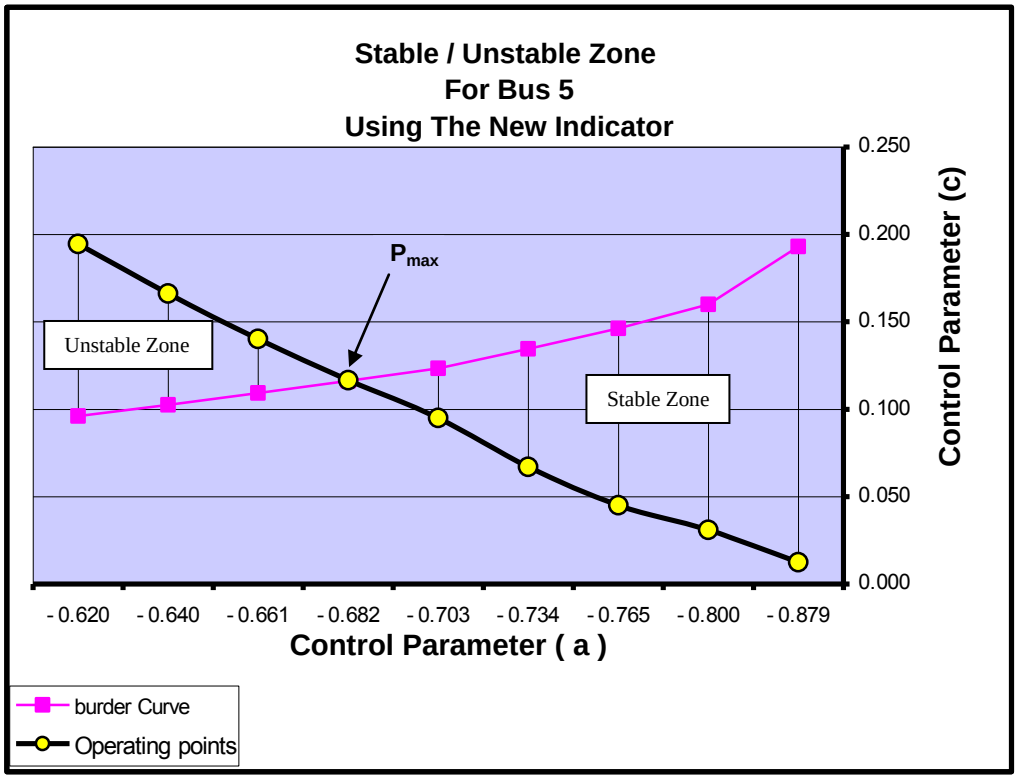

Figure 5-c: Operating Zones for Bus 5.

Table 5-d: The New and Different Voltage Stability Indicators for Load Bus 6 for 6 – Bus Power System.

Bus Number	New indicator		Jacobian Value $\lvert J_x \rvert$	Eigenvalue λ	Critical Voltage V_{cr}	Bus Loading	System State
	c	a					
BUS 6 Maximum Loading p.u 1. 5357	0.0149	-0.902	0.205823	4.216143	0.663	Base Load	Stable
	0.0350	-0.862	0.184078	3.949922	0.648	50% P_{max}	Stable
	0.0503	-0.839	0.168060	3.709058	0.639	60% P_{max}	Stable
	0.0786	-0.805	0.136814	3.159393	0.626	75% P_{max}	Stable
	0.1132	-0.770	0.088957	2.169858	0.613	90% P_{max}	Stable
	0.1397	-0.748	0.000000	0.074827	0.603	100% P_{max}	Critical Stable
	0.1690	-0.724	-0.35550	-8.825145	0.594	110% P_{max}	Unstable
	0.2011	-0.702	-0.35550	-9.108338	0.585	120% P_{max}	Unstable
	0.2360	-0.679	-0.35550	-9.410307	0.575	130% P_{max}	Unstable

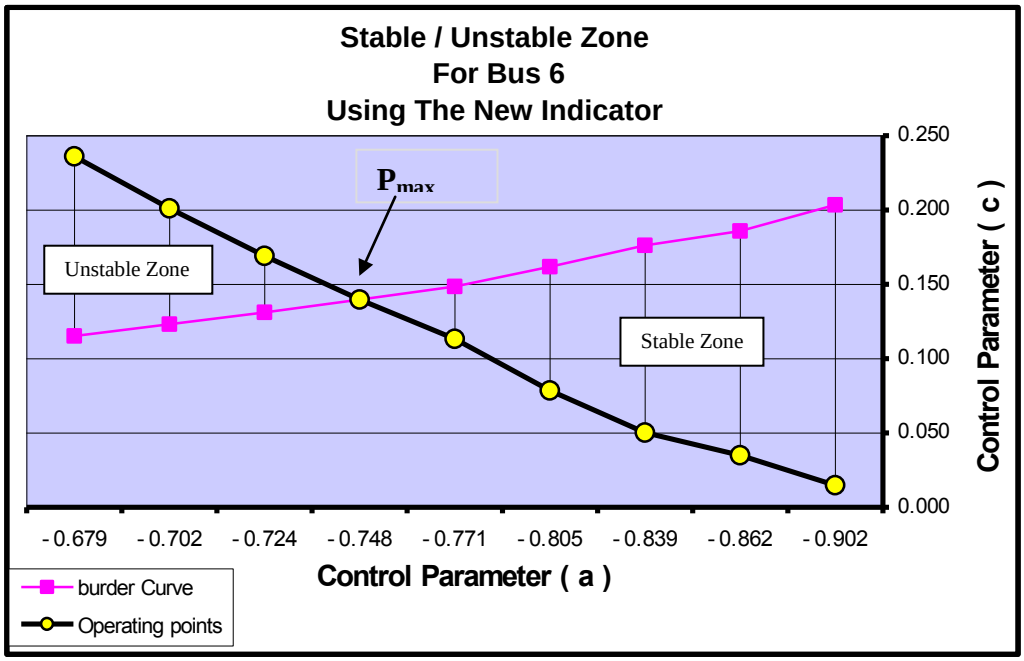

Figure 5-d: Operating Zones for Bus 6.

6.2 The Second Test

As illustrated in **Table 5-c** the values of the control parameter c of bus 5 as compared to the other buses are the smallest values as well as its eigenvalues obtained. Therefore bus 5 is considered here the weakest bus in the system. In order to test the three criteria

for this bus with load active power is kept constant at 0.3 p.u and load reactive powers are assumed to be increased gradually from 0.18 p.u up to 402.8 % of its nominal value i.e reactive power of that bus is increased to 0.725 p.u. The node critical voltages nearly dropped down by 25 % from stable to unstable cases.

The criteria for the system to be stable, the new indicator c should be less than $(a/2)^2$, the determinant values of the Jacobian $|\mathbf{J_x}|$ and the eigenvalues λ also should be positive values as shown in **Table 6**. As shown in **figure 6** the break away point which represents the critical reactive power loading point at bus 5 occurs at 0.715 p.u . This agree with the given results .

Table 6: The New and Different Voltage Stability Indicators for Bus 5 at different Loading VARs With Constant Active Power 0.3 p.u.

Bus Number	New indicator		Jacobian Value | Jx |	Eigenvalue λ	Critical Voltage Vcr	Bus 5 VARs p. u	System State
	c	a					
BUS 5 Base Loading p.u 0.3	0.01040	-0.87865	0.276166	2.936918	0.6630	0.18	Stable
	0.02229	-0.71861	0.210677	2.201371	0.6000	0.36	Stable
	0.03890	-0.60795	0.148268	1.530762	0.5510	0.54	Stable
	0.05080	-0.44281	0.103353	1.060713	0.5260	0.63	Stable
	0.06200	-0.50359	0.024072	0.245756	0.5020	0.710	Stable
	0.06230	-0.50239	0.018062	0.184371	0.5010	0.712	Stable
	0.06240	-0.50159	0.014128	0.144204	0.5009	0.713	Stable
	0.06260	-0.50119	0.008541	0.087175	0.5006	0.714	Stable
	0.62700	-0.50040	-0.161575	-1.501579	0.5003	0.715	Unstable
	0.63500	-0.49719	-0.161575	-1.500193	0.4988	0.720	Unstable
	0.06420	-0.49437	-0.161575	-1.498810	0.4972	0.725	Unstable

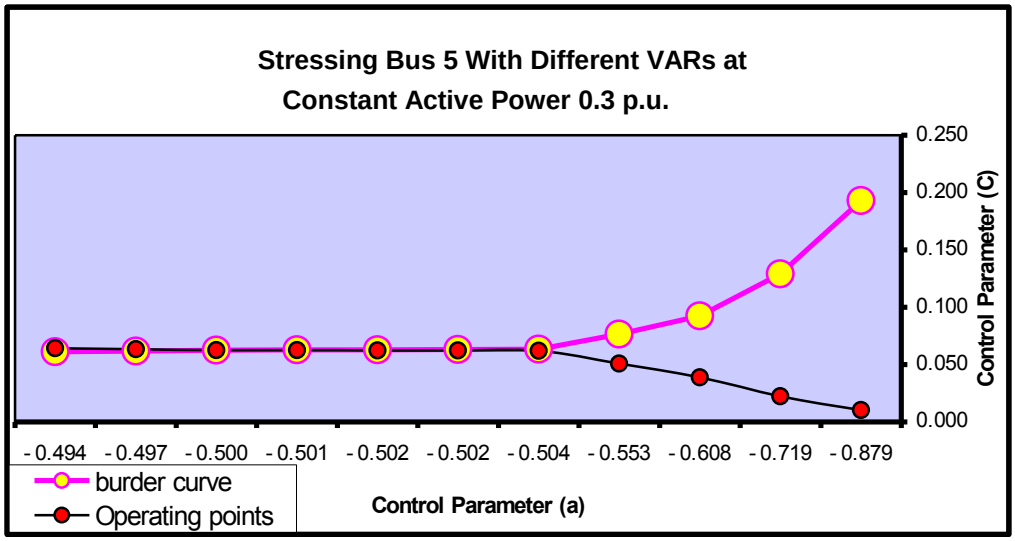

Figure 6: Operating Zones for Bus 5 at Different VARs With Constant active Power.

7- CONCLUSIONS

1. This paper has developed a new voltage stability indicator for integrated power systems using the catastrophe theory.
   A swallowtail manifold has been shown to be appropriate for this new indicator.
2. An algorithm has been presented in this paper and a developed C – language program is used to calculate the new indicator in terms of the system parameters; load active and reactive powers, transmission impedance, and the voltage source . These system parameters can be measured or calculated with a speed adequate for on-line steady-state voltage stability assessment. It has been shown that the zone inside the border curve which represents the curve of critical points and the curve of bus operating points represents the steady voltage stable zone, and the voltage collapse occurs in the zone that produced after the system is loaded with value greater than maximum load P_{max}.
3. Coincidence of the obtained results of the new indicator, determinant of the Jacobian, and the eigenvalues is proved for system load nodes of different active and reactive power loadability conditions leading to stable and unstable voltage cases.

8 – REFERENCES

[1] T. Nagao, " Voltage Collapse at Load ends of Power Systems " Electrical Engineering in Japan, Vol. 95, No. 4, 1975.
[2] W.R. Lachs, " Voltage Collapse in EHV Power Systems " , paper No. A 78 057-2, IEEE PES, winter power meeting, Jan/Feb 1978.
[3] M.Z. El-Sadek, " Preventive Measures for Voltage Collapses and Voltage Failures in the Egyptian Power Systems ", Electric Power Research, Vol. 44, No. 3, 1988.
[4] M.Z. El-Sadek, " Prevention of Repetitive Blackouts in the Egyptian Power Systems ", 2nd MEPCON 1992, Assuit University, Egypt, pp. 14-19, Jan.1992
[5] T.V. Cutsem, " Dynamic and Static Aspects of Voltage Collapse ", Proc. of Eng. Found. Conf. on bulk power system voltage phenomena – voltage stability and security, Potosi, Mi, Sept. 1988, pp 655-679.
[6] B. H. Lee, and K.Y. Lee " Dynamic and Static Voltage Stability Enhancement of Power Systems ", IEEE Trans on power system, Vol. 8, No. 1, Feb 1993, pp 231-283.
[7] V.Ajjarapu, "Identification of Steady-State Voltage Stability in Power Systems" Vol. 11, No.1, 1991, pp 43-46.
[8] V.Ajjarapu, and C. Christy, " The Continuation Power Flow: a tool for steady-state voltage analysis ", IEEE on power systems, Vol. 7, No.1, Feb 1992, pp 416-423.
[9] B.Gao, G.Morison and P.Kundur, "Voltage Stability Evaluation Using Modal Analysis ", Trans on power system, Vol. 7, No. 7, Nov. 1992, pp 1529-1542.
[10] N. Amjady, and M. Esmail, " Application of a New Sensitivity Analysis Framework for Voltage Contingency Ranking ", IEEE Trans. On power systems, Vol. 20, No. 2, May 2005, pp 973-983.

[11] S. Greene, I. Dobson, and F. L. Alvarade, " Sensitivity of the loading margin to voltage collapse with respect to arbitrary parameters ", IEEE Trans. On power systems, vol. 12, No. 1, Feb. 1997, pp 262-272.
[12] J.L. Dineley and G. A. Mahmoud, " A New Method of on-line Evaluation of Synchronous Power System Stability ", IEE 2nd international Conference on Power Monitoring and Control, 1986, pp 333.
[13] G. A. Mahmoud, " Study of Voltage Instability in Power Systems Using Catastrophe Theory ", Mansoura Engineering Journal (MEJ) Vol. 17, No. 4 Dec. 1992.
[14] T.Poston, and I.Stewart,"Catastrophe Theory and its Application",Pitman, London, 1978.
[15] R. Gilmore,"Catastrophe Theory for Scientists and Engineers", Wiley, New Yourk, 1981.
[16] E.C. Zeeman, "Catastrophe Theory ", Scientific American, April 1976, pp 65-83.
[17] M.Z. El-Sadek, " Power System Voltage Stability and Power Quality ", Mukhtar Press, Assuit, Egypt 2002.
[18] W.M. Wang, J.F. Chen and C.L. Huang, " Analysis of Stability and Uniqueness of Load Flow Solution of Radial Distribution Systems ", Inter. Power Eng. Conf. 1993, March, Singapore, pp 119-124.
[19] V.A. Venikov, V. A. Stroev, V.I. Idelechick, and V. I. Tarasov, " Estimation of Electrical Power System Steady-State Stability in Load Flow Calculation ", IEEE Trans. On PAS, Vol. PAS-94, No. 3, pp 1034-1041 May/Aug 1975.
[20] S. Abdelkader, "Transmission Loss Allocation in Deregulated Electrical Energy Market" , 10 th MEPCON, Dec. 2005, Port-Said, Egypt, pp 733-739.

مؤشر الاقتراب الجديد لانهيار الجهـــد

لقد أصبحت مشاكل الاتزان فى الجهد لشبكات القوى الكهربية واحدة من أكبر اهتمامات مرافق تقديم الخدمات الكهربية.

هذا البحث سجل طريقة جديدة لمؤشر الاقتراب لحالة الانهيار في الجهد مستخدماً نظرية النكبة مقارنة مع الطرق التقليدية المستخدمة في هذا المجال: مثل الطريقة المفردة **(Singularity)** لمحدد مصفوفة الجاكوبيان لتدفق الطاقة الكهربية وكذلك طريقة التحليل الناقص **(Modal analysis)**. أوضحت هذه الطريقة وسيلة لتعيين منطقة التشغيل المتزنة لشبكات القوى الكهربية، وكذلك النقطة الفاصلة التي بعدها يحدث الانهيار في جهد تشغيل النظام. تمت الدراسة على شبكة كهربية **Ward-Hale 6-bus Network** مستخدما مكافئ **Thevenin** لهذه الشبكة عند فصل قضبان التحميل كلا على حدة.

النتائج التي تم التوصل إليها في هذه الدراسة أعطت التطابق التام في جميع حالات التحميل، حيث أعتبر المؤشر الجديد حالة التشغيل في منطقة الجهد المتزن تحدث عندما

تكون قيمة c موجبة وأقل من $(a/2)^2$ وهو ما يتطابق مع قيمة محدد مصفوفة سريان الطاقة الموجب وكذلك القيمة الموجبة للـ **Eigenvalues**

تم إجراء اختباران على الشبكة المستخدمة : الاختبار الأول تم فيه تحميل قضبان الأحمال المختلفة بقيم للقدرة الفعالة تصل إلى 130 % من الحمل الأقصى الذي تم استنتاجه خلال هذا البحث مع فرض مركبة القدرة الغير فعالة لهذه الأحمال ثابتة لا تتغير، حيث كانت النتائج التي تم الحصول عليها تتطابق مع الطرق التقليدية الأخرى . أما الاختبار الثاني فقد تم فيه الدراسة على القضبان الواهنة التي تم تحديدها أيضا في هذا البحث وتحميلها بأحمال ذات قدرة فعالة ثابتة القيمة وبقدرة غير فعالة متغيرة القيمة, وأيضاً أمكن تحديد منطقة التشغيل المتزنة وكذلك النقطة الفاصلة التي بعدها يحدث الانهيار في جهد تشغيل النظام مما يعطى لهذا المؤشر الجديد إمكانية التطبيق العملي والمراقبة الفورية لمناطق تشغيل قضبان التحميل بشبكات القوى الكهربية.